

RSC Advances



This is an *Accepted Manuscript*, which has been through the Royal Society of Chemistry peer review process and has been accepted for publication.

Accepted Manuscripts are published online shortly after acceptance, before technical editing, formatting and proof reading. Using this free service, authors can make their results available to the community, in citable form, before we publish the edited article. This *Accepted Manuscript* will be replaced by the edited, formatted and paginated article as soon as this is available.

You can find more information about *Accepted Manuscripts* in the [Information for Authors](#).

Please note that technical editing may introduce minor changes to the text and/or graphics, which may alter content. The journal's standard [Terms & Conditions](#) and the [Ethical guidelines](#) still apply. In no event shall the Royal Society of Chemistry be held responsible for any errors or omissions in this *Accepted Manuscript* or any consequences arising from the use of any information it contains.

Saturation of two photon emission in ZnO nanoparticles with second order nonlinearity

J. Lin¹, Y. Fujita,* A. Neogi¹

¹Department of Physics, University of North Texas, Denton, TX, USA 76203

²Faculty of Interdisciplinary Sciences, Shimane University, Matsue, Japan

Abstract:

The nonlinear optical effects such as second harmonic generation and two-photon emission in ZnO nanocrystals have been studied using microscopic time-resolved and time-integrated emission spectroscopy. The two-photon emission efficiency is proportional to the emission from defect level. The stimulated transition of the carriers from the conduction band-edge to the defect states significantly influences the efficiency of the two photon process. The nonlinear emission characteristic depends significantly on the origin of the emission and the power dependence is significantly different from the surface emission compared to that emitted within the bulk of the nano-crystal. The two photon emission efficiency generated within the bulk semiconductor reduces at higher pump photon densities due to the saturation of the defect level states populated by stimulated emission. The two-photon emission from the surface of the ZnO nanocrystals increases and then followed by a saturation due to the increase in the intensity. Unlike the two-photon emission from the bulk of the crystal, the surface emission does not show any drop in the efficiency at higher pump intensities.

* Corresponding Author: arup@unt.edu

The nonlinear optical properties of ZnO nanocrystals including nanoparticles [1,2], nanowires [3], nanorods [4,5] and quantum dots [6] have garnered increasing interest due to their potential application in UV emitters [4,6] and biomarkers [2,7,8] for optoelectronics and biomedical imaging. ZnO is a non-centrosymmetric (NCS) semiconductor which facilitates quadratic nonlinearities such as second harmonic generation [2,5,9], or optical rectification [10] process. However, cubic nonlinear effects such as two- or multiphoton emission [1,7-10] also occur concurrently with second order nonlinear processes within the ZnO lattice. ZnO is a direct bandgap semiconductor with a relatively strong exciton binding energy (~ 60 meV) compared to most direct bandgap semiconductors. The linear interband transition and the resulting light emission process in the presence of excitonic states along with several below band gap states due to shallow and deep defects makes the light emission process rather complex. [11] ZnO also has a large exciton oscillator strength and wide-spread LO phonon energy (72 meV at 5 K). The selection rule for multiphoton absorption process in ZnO can be rather complex and thereby effects the two-photon emission spectrum.

From a quantum mechanical perspective, the retardation effects due to the lack of inversion symmetry in ZnO lattice, accentuated by the defects such as oxygen vacancy or Zn interstitial sites can be very significant [12]. The photoluminescence emission due to two-photon absorption is usually more efficient when the two-photon excitation energy is around half the bandgap of the semiconductor due to enhanced third order optical nonlinearity. [12,13] However, the NCS affects the $\chi^{(3)}$ of the system especially for near-bandgap resonant transition regime. The effect of non-centrosymmetry of the medium on the third order optical nonlinearities for band-edge resonant transitions is more significant in polar semiconductors like ZnO due to the modification of the electron-LO coupling. One possible way is to explore the frequency and power dependence of the two-photon emission process in the presence of second harmonic generation. Recently there are a few reports on the competitive effects of SHG and two-photon emission process in nanoparticles [1,9,14-15]. The excitation density dependence of the nonlinear process has been analyzed and has usually been observed to increase with the pump-intensity for the two-photon emission process [9,15] and the second harmonic generated light and eventually saturate for the latter [9]. The nonlinear system is usually observed to be dominated by the third-order nonlinear process at higher excitation density and has been interpreted in terms of the thermal dissipation and electric field distribution. In all these reports, the measurements were performed at room temperature. The presence of phonons at room temperature does not influence the macroscopic SHG process, however the two-photon process is significantly influenced. Almost none of the work on optical nonlinearity in ZnO nanocrystal system has reported the two-photon absorption induced radiative recombination rate. The competition of the SHG and two-photon process is also very unique. The novelty of the work arises from the change in the two-photon process depending on the origin of the process and the excitation conditions. The characteristics

of the two-photon induced nonlinearity, such as the absorption saturation behavior or the recombination lifetime is distinctively different when the emission occurs from within the bulk or from the surface of the nanocrystals. In the present paper we investigate the optical nonlinearities at low temperature especially the two-photon emission process in the ZnO nanocrystals. The origin of two-photon nonlinearity in the presence of second harmonic generation is discussed in the present paper. The dependence of radiative lifetime on the excitation density is also presented that has not yet been investigated. A tunable laser source has been used to study the induction of the optical nonlinearity both at the band-edge resonance and also at off-resonant frequencies. The effect of the defect level states on the two-photon emission process has been studied. The excitation density dependence studies has been corroborated with time-resolved emission spectroscopy measurement at 4.2 K.

ZnO nanocrystals, in powder form, were synthesized using an arc plasma method [1] at atmospheric pressure in an air ambient with an arc current of 90 A) and were then annealed in atmosphere at 1000° C for 1 hour. [1]. The ZnO crystals in nano- and micro-scale was optimized with enhanced two-photon emission properties by growing them in atmospheric air with high crystalline quality and with relatively low oxygen vacancy in the lattice. The nanocrystals had surface that were highly positive in nature. The shape of the ZnO particles ranged arbitrarily from nano- and micro-particles to tetrapods as shown in Figure 1a.

The nonlinear optical measurement were performed using a 40x objective lens with long working distance to couple the light into a cryostat. The SHG measurement were performed under a collection geometry with the SHG signal being collected in the forward direction, where as the two-photon emission measurement were performed under an illumination-collection geometry. A tunable Ti:Sapphire laser source(690nm to 960nm) with pulse width 80 fs and a repetition rate of 80 MHz was used as the excitation source. The two-photon PL emission was detected by a Streak Camera (Hamamatsu Streak Scope C4334) with a resolution of 15 ps. A closed cycle liquid Helium cryostat was used for maintaining the samples at 4.2 K. For the single photon photoluminescence measurement, a BBO crystal based frequency doubler was used with the excitation wavelength at 350 nm. We also used a CW HeCd laser source with the excitation wavelength at 325nm for steady-state PL measurements.

Figure 1b shows the PL spectrum due to single photon excitation by 350nm laser pulse at 3mw to induce emission from free excitons at 3.29eV nm and an exciton bound to Zn interstitial atom at 3.22 eV and a broad peak from defect levels centered around 2.9 eV. However, no green emission was observed from these samples due to the presence of any oxygen vacancy as widely prevalent in wet chemistry based synthesis techniques. The penetration of the incident light at 350 nm is ~50 nm within the nanocrystal, which is significantly lower than infrared irradiation at 700 nm or at 800 nm. The excitation by

the near-infrared laser at 800 and 840 nm results in SHG at 400 and 420 nm. The width of the SHG signal is dictated by the width of the fundamental pulsed laser. The SHG signal is simply a harmonic output of the input laser source and manifests the width of the 80 fs excitation pulse that has a transform limited width of ~ 14 nm at 800 nm. The SHG signal can be clearly observed for a pump wavelength corresponding to 750 nm. However, a further reduction of the excitation wavelength results in interband transition due to two photon excitation.

Figure 1c shows the two-photon emission spectra at various excitation power at 4.2 K with the excitation energy at 730nm (1.7 eV) with the energy high enough to enable band-band transition in ZnO ($E_g \sim 3.37$ eV) via a two-photon absorption process. It is observed that an emission at 383 nm is observed accompanied by a broad band emission from 400-470 nm. As the excitation density is increased, the high energy emission red-shifts and merges with the blue emission at ~ 430 nm. Phonon assisted multi-photon transition is likely to be responsible for the emission from states significantly below the bandedge of the ZnO or the single photon PL emission.

Figure 1d shows a comparison of the single photon and two-photon induced photoluminescence process excited by low and high power incident laser excitation. The sharp excitonic emission observed under single photon excitation at 3.81 eV or 325 nm light is not observed in the multi-photon process induced emission. There are two reasons for the application of high excitation power densities for the study of the multi-photon process. Firstly the two photon absorption process is a nonlinear process and occurs at relatively higher threshold compared to single photon process. Due to very low two-photon cross-section in ZnO nanocrystals, one cannot observe the two-photon induced PL emission at very low excitation densities which has been used to observe single photon PL. The density of state in the conduction band which mediate the single photon absorption is significantly higher compared to the virtual states or the deep-level defect states which mediate the two-photon absorption process.

Secondly as a high-repetition rate frequency doubled Ti:Sapphire laser is used, it is impossible to obtain comparable or very high power densities in the UV range for single photon excitation process. On the other hand the Ti:Sapphire laser fundamental wavelength used for the two-photon or SHG process has significantly higher excitation power. Moreover as we have used a microscope objective to differentiate the surface and bulk or volume excitation in the ZnO nano-crystals it is impossible to reduce the power to the level of single photon excitation using CW HeCd laser or second harmonic laser excitation.

The penetration of the excitation light pulses at wavelength ~ 350 nm is significantly shorter than the excitation at 730 nm. This is not only due to the lower penetration of the short wavelength light within a dielectric compared to the longer

wavelength light, but also there is no linear absorption of the photon incident at 730 nm. Moreover the shorter wavelength light generated within the ZnO crystals due to the band-edge emission are reabsorbed within the nanocrystal which is more than the single photon induced PL that occurs mostly at the surface. It leads to a quenching of the short wavelength emission which is significantly more in case of two-photon process resulting in a quenching of the high energy emission. The peak center of the two-photon emission thereby appears to be red shifted. [17]. The thermal effects are dominant at room temperature. All the experimental results presented in the present work were performed at 77 K or lower. At low temperature the thermal effects appears do not affect the emission process as the recombination lifetime is observed to be longer. Any thermal induced phonons will result in dissipative process which will increase the non-radiative recombination rate and thereby reduce the PL lifetime and is not observed in our case. In fact the recombination lifetime of the two-photon induced recombination process increases with intensity due to the many-body effects and the hole-state mediated recombination process.

Figure 2a shows the comparison of the SHG and TPE efficiency as a function of the excitation laser wavelength. It is observed that the two-photon process and the second harmonic generation process compete with each other from 700-760 nm wavelength. When the wavelength was above 760nm, the SHG process dominated; whereas for wavelength below 750 nm the two photon emission process dominated. Between 745-755nm the efficiency of the SHG and the two-photon process is almost identical. The experimentally measured absorption coefficient for the ZnO nanocrystals is shown in Figure 3 (b).

The SHG always occurs in ZnO crystals due to the surface and the non-centrosymmetric nature irrespective of the excitation wavelength. However, as we approach the excitation wavelength to 750nm and below, the two photon absorption below bandgap occurs due to presence of defect states. The SHG light is absorbed by ZnO crystal. This band-edge absorption modified the light matter interaction and the SHG generation efficiency as well. This is also the possibility of SHG induced band-edge photoluminescence which can contribute to the total emission process.

The relative increase in the two-photon efficiency can be explained using the uncertainty principle, where $\Delta E \cdot \Delta t > h$, where $\Delta E (= E_{ex} - E_g)$ is the difference between the incident photon energy and the bandgap of the semiconductor and Δt is the lifetime of the virtual state. The smaller ΔE (or in other words, for resonant two-photon excitation) the longer is the lifetime of the virtual state. Therefore the carriers in the virtual state will have more probability of interacting with the incident light and absorb the second photon to be excited into the conduction band resulting in a higher two-photon efficiency. Thus the two-photon transition rate increases with an increase in the incident light energy (frequency).

On the other hand as the excitation wavelength increases, the two-photon absorption decreases and the nonlinearity in the NCS ZnO crystal is dictated by second harmonic generation. The SHG emission is dominant for excitation wavelength above 750nm. The SHG conversion efficiency increases with the wavelength due to the increase in the penetration depth of the photons within the crystal as well as reduced scattering compared to photons at shorter wavelength.

The second harmonic generation always occurs in the ZnO nanocrystals due to the surface and the non-centrosymmetric nature of the crystal irrespective of the excitation wavelength. In results which is not show in the present paper we have observed second harmonic generation using NIR laser even at wavelengths exceed 1.0 micron using Nd:YAG lasers. However on the use of excitation wavelengths lower than 750 nm, the two-photon absorption below the bandgap occurs due to the presence of defect states such as Zn interstitials. The generated SHG light is absorbed by the ZnO nanocrystal. Using separate studies, using high resolution microscopy we have observed SHG in the presence of two-photon emission. As one gets to the lower wavelength such as 720nm or below, the SHG is not only absorbed by the bandgap of the semiconductor. This band-edge absorption by the semiconductor in turn modifies the light matter interaction and the SHG generation efficiency as well. There is also the possibility of SHG induced bandedge photoluminescence which can contribute to the total emission process.

So the competition of SHG and two-photon emission process occurs due to the flow of energy from simply non-absorption two-wave mixing (SHG process below the bandgap) to three-wave mixing process in the two-photon absorption of light associated with one photon emission close to the semiconductor bandgap. A temperature dependence of the PL and second harmonic generation process was studied. The PL intensity increases with a decrease in temperature as the non-radiative processes due to phonon scattering are minimized. The modification of electron-phonon coupling also increases the emission efficiency from the bandedge exciton. The SHG intensity is however independent of the temperature and depends more on the surface scattering properties of the ZnO nanocrystal which can be effected by the nano-particle aggregation.

Figure 3 depicts the power dependence of the TPE process in ZnO nanoparticles. The two-photon absorption coefficient usually increases with incident power densities, but eventually attains a saturation [20] at higher photon densities. However we have observed that the saturation behavior strongly depends on the origin of the two-photon emission. Figure 4a shows the power dependence of TPE from within the volume of the ZnO nanoparticles. The intensity dependence of the total TPE process is compared with the power dependence of the stimulated emission mixed with electron-hole-plasma (SMEHP) emission and defect bound excitonic emission in the ZnO semiconductor nanocrystals. [18, 19].

Initially, there is an increase of the two photon process along with the stimulated (SMEHP) and defect emission. However as the electron density increases, the defect emission due to Zn interstitial is saturated and the total emission decreases significantly along with the stimulated (SMEHP) process. This decrease in the TPE can be altered by focusing the light to the surface of the ZnO nanocrystals where the total absorption of the total number of incident photons within the semiconductor is limited to the surface. Figure 3b shows that the unlike the emission characteristics from within the nanocrystal, the effective TPE from ZnO surface increases. This increase is not due to change in the non-radiative recombination process due to reduced surface traps as in case of single photon photoluminescence as it can be observed from Fig.3b that the defect density did not saturate and instead increased at higher power. However, the TPE characteristics from the stimulated electron-hole plasma (SMEHP) emission process and the is similar to that of the TPE emission from within the bulk of ZnO nanocrystals. The difference in the behavior of the defect emission is likely due to the location of the defects within the ZnO nanoparticles compared to its interaction with the photons. TEM analysis [1] shows high crystalline quality within the bulk of the samples with low defect density which are saturated easily compared to relatively higher defect at the surface that takes more photons to saturate. Thus for the laser power used for the current experiment with nano-Joule of energy, the Zn interstitial defect are not saturated and any increase of the photon density actually increases the defect bound excitonic recombination as well as the two-photon transition probability.

In case of two photon emission in ZnO nanoparticles, the carriers excited into the virtual state absorbs a second pump photon and are pumped into the conduction band. When the photon density is low as in case of a weak excitation intensity, the excitons or the carriers occupy those state corresponding to the double of the incident energy or subsequent lower energy states. However, there are two components emission spectrum excited by a 730 nm laser source- the free exciton emission and electron hole plasma recombination. With an increase in pump intensity, the electron hole plasma dominates the TP emission spectrum and is consequently redshifted.

Figure 4 shows a schematic of the decay process in our system. As in case of any two-photon process, the electrons from the valence band absorb an incident photon and is excited to the virtual state and re-excited to the conduction band instantly on the absorption of a second photon. The emission can occur due to the recombination of the excited carriers from the conduction band with the holes in the valence band with an energy ~ 3.3 eV. At high enough excitation densities, the carriers can emit due to stimulated (SMEHP) emission in the range 3.2 -3.05 eV [21-23]. The presence of Zn vacancy sites at 0.2 eV above the valence band can result in additional defect level emission that can be significantly red-shifted [24]. The carriers can non-radiatively decay to the defect level states. For lower excitation photon density, excitonic states are not saturated and free exciton can dissociate and relax to other allowed defect bound excitonic eigenstates. However under stronger optical pump intensity, the lower energy states in the CB are likely to be fully occupied due to band-filling effect. It results in

reduced carriers from the intermediate virtual state to the conduction band, which can lead to a decrease of hole density in the valence band.

Figure 5a shows the time-resolved photoluminescence lifetime for the single photon, two-photon process along with the temporal profile for the second harmonic signal. As mentioned earlier, the SHG process is dictated by the femtosecond pulse profile and the temporal resolution is limited by the speed of the streak camera. The emission life-time from both the single and two-photon excitation process is measured. It should be emphasized that the measurements were performed at low temperature (4.2 K) so that the non-radiative recombination process due to phonon scattering can be minimized. The band-band recombination process is observed to be a bi-exponential process (Fig. 5a), with the faster process being the non-radiative process with a shorter time constant t_1 , whereas the slower process being the radiative process with a relatively longer time constant t_2 . The faster process is comparable for both the single and two-photon process with $t_{1-(PL)} \sim 0.14$ ns, whereas $t_{1-(TPE)} \sim 0.13$ ns. The radiative lifetime on the other hand is significantly more longer for the single photon induced PL process ($t_{2-(PL)} \sim 3.12$ ns) as compared to the two-photon induced emission process ($t_{1-(TPE)} \sim 1.56$ ns). Compared to single photon process, the two-photon process is influenced more by exciton-phonon interactions which modifies the radiation recombination rate. Localization of excitons in semiconductors usually results in increased radiative lifetime with binding energy [25]. The red-shift in the two-photon transition induced emission spectrum along with the relatively shorter radiative lifetime is an indication of delocalized excitonic or defect bound excitonic contribution to the emission process.

Figure 5b shows the time-resolved two-photon emission at low and high intensities. It can be observed that decay time increases with the incident power density. The carrier screening induced by the increased pump-photon density is likely to increase the recombination lifetime. For off-resonant two-photon excitation well above the band-edge the trapping of the photo-carriers by deep level defect center at the mid-gap can also reduce the carrier recombination time. The wave vector difference is doubled in the two-photon excitation process, which results in the participation of phonons in the recombination process as evidenced by the large red-shift in the emission spectrum. This results in an increase in the recombination lifetime for the electron-hole plasma as shown in Figure 5b. The two-photon emission decreases due to the reduced probability of electron-hole plasma even though the Zn interstitial vacancy states are not affected by the band filling effect in the conduction band.

In conclusion, we present an experimental analysis of the competition of two-photon process in a noncentrosymmetric medium with high SHG efficiency. It is observed that the below bandgap states significantly influence the efficiency of the two-photon process. It is observed that the SHG process is more efficient at higher pump wavelength, and is

completely dominated by the two photon emission process below 750 nm. The two-photon emission is optimal when the incident photon density is localized close to the surface of the ZnO nanoparticles. At high pump intensities, the re-absorption of the UV visible light by the Zn interstitial defect sites leads to the decrease of two photon emission generated within the bulk of the nanocrystals.

References:

- [1] Urban B. E., Lin J., Kumar O., Senthilkumar K., Fujita Y., and Neogi A., 2011, *Opt. Mater. Express* **1**, 658.
- [2] Urban B. E., Neogi P. B., Butler S. J., Fujita Y., and Neogi A., 2012, *J Biophotonics* **5**, 283.
- [3] Johnson J. C., Yan H., Schaller R. D., Petersen P. B., Yang P. D., and Saykally R. J., 2002, *Nano Lett.* **2** 279.
- [4] Dai J., Fu Z., Lan S., Wan X., Tie S., Trofimov V. A., and Lysak T. M., 2012, *J. Appl. Phys.* **112**, 063102.
- [5] Liu S. W., Zhou H. J., Ricca A., Tian R., and Xiao M., **2008**, *Phys. Rev. B* **77**, 113311.
- [6] Chattopadhyay M., Kumbhakar P., Tiwary C. S., Mitra A. K., Chatterjee U., and Kobayashi T., 2009, *Opt. Lett.* **34** 3644.
- [7] Trunina N. A., Popov A. P., Lademann J., Tuchin V. V. Myllylä R., Darvin M. E., 2012, *Proc. SPIE 8427, Biophotonics: Photonic Solutions for Better Health Care III*, 84270Y
- [8] Wu Y. L., Fu S., Tok A. I. Y., Zeng X. T., Lim C. S., Kwek L. C., and Boey F. C. Y., 2008, *Nanotechnology* **19**, 345605.
- [9] Dai J., Zeng J.H., Lan S., Wan X., and Tie S.L., 2013, *Optics Express*, **21**, 10025
- [10] Minimala N.S., John Peter A., 2012, *Journal of Nano- & Electronic Physics*; **4** , 04004.
- [11] Ozgur U., Hofstetter D., and Morkoç H., 2010, *Proceedings of the IEEE*, **98**, 1255.
- [12] Sen P., Sen P.K., 1985, *Phys. Rev. B.*, **31**, 1034.
- [13] Boyd R. W., 2008, *Nonlinear Optics*, 3rd ed. Academic Press.

- [14] Deng H. D., Li G. C., Dai Q. F., Ouyang M., Lan S., Trofimov V. A., and Lysak T. M., 2013 *Nanotechnology* **24**, 075201.
- [15] Han N. S., Shim H. S., Park S. M., and Song J.K., *Bull. Korean Chem. Soc.*, **30**, 2199 (2009).
- [16] Ozgur U., Morkoc H., 2009, "Zinc Oxide: Fundamentals, Materials and Device Technology" by Umit Ozgur, Hadis Morkoc", WILEY-VCH .
- [17] Foreman J., Everitt E., *Phys. Rev. B* 2010, **81**, 8765
- [18] U. Ozgur, A. Teke, C. Liu, S. Cho, and H. Morkoc; *Appl. Phys. Lett.*, 84, #17, 3223, 2004
- [19] T. C. He, R. Chen, W. W. Lin, F. Huang and H. Sun; *Appl. Phys. Lett.*, 99, 08102, 2011
- [20] Vivas M.G., Shih T., Voss T., Mazur E., and Mendonca C. R., 2010, *Optics Express*, 9628.
- [21] Guillet T., Brimont C., Valvin P., Gill B., Bretagnon T., Médard F., Mihailovic M., Zúñiga-Pérez J., Leroux M., Semond F., and Bouchoule S., 2012, *Phys. Stat. Solidi* **C9**, 1225.
- [22] Zu P., Tang Z. K., Wong G. K. L., Kawasaki M., Ohtomo A., Koinuma H., and Segawa Y., 1997 *Solid State Commun.* **103**, 459.
- [23] Bagnall D. M., Chen Y. F., Zhu Z., Yao T., Shen M. Y., and Goto T., 1998 *Appl. Phys. Lett.* **73**, 1038.
- [24] Sreeja R., John J., Aneesh P.M., Jayaraj M.K., 2010 *Optics Commun.* **283**, 2908.
- [25] Chen G.D., Smith M., Lin J.Y., Jiang H.X., 1996 *Appl. Phys. Lett.* **68** 2784.

Figure captions:

Figure 1a-i Transmission electron microscope (TEM) images of ZnO nanoparticles
a-ii Scanning electron microscope (SEM) image of ZnO

Figure 1b: Photoluminescence spectrum from ZnO nanocrystals with input laser wavelength at 350 nm and the normalized second harmonic generated signal with the excitation laser at 740nm, 800nm and 840nm

Figure

(1c) Two photon emission spectrum with the laser spot at the surface (near surface) with an excitation laser wavelength at 730nm laser pulse at various average incident power.

Figure (1d): Comparison of photoluminescence emission spectrum - the single photon PL is observed due to excitation by 356nm laser at 3mw and two photon emission excited by 730nm laser at 510mw and 1170 mw. The internal figure is SMEHP peak position shifted with incident power.

Figure 2:

(a): Normalized Intensity I_{out}/I_{in} for Two photon emission and second harmonic generation

(b): Absorption coefficient for ZnO nano-particles.

Figure 3:

Intensity dependence of two-photon emission on the incident laser intensity. The solid triangle represents total emission; solid round represents SMEHP emission and solid square represents defect emission.

(a) Two photon emission from within the ZnO nano/microcrystallites.

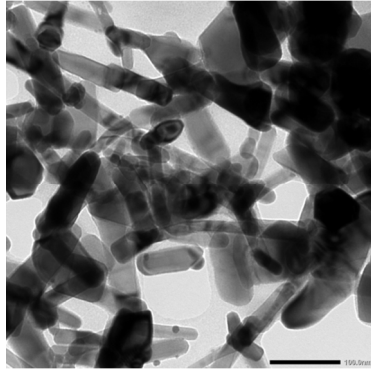
(b) Two photon emission from near surface of ZnO nano/microcrystallites.

Figure 4: Schematic ZnO two photon emission process. The double thin solid lines represents two photon excitation; the thick single solid line is the Bband emission (BE); a single dashed line is the SMEHP emission (SE) and double dashed line represents defect emission (DE). V_{Zn} is Zn vacancy

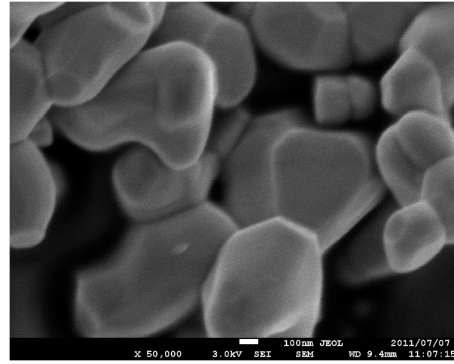
Figure 5a: Comparison of single photon PL, two-photon emission and SHG intensity

Figure 5b: Two photon emission decay time depend on incident power intensity

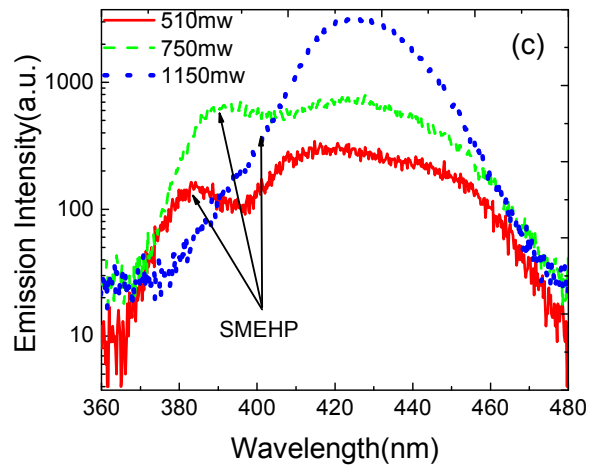
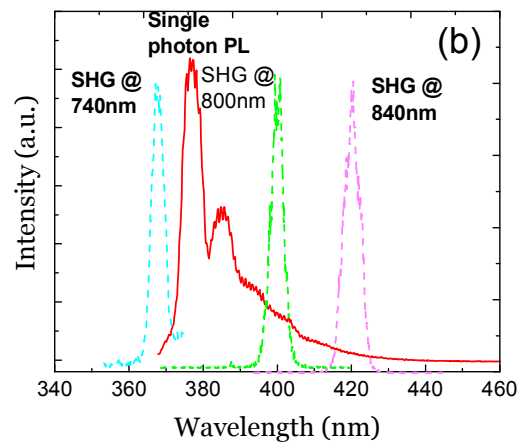
Figure 1: Lin et al.



(a-i)



(a-ii)



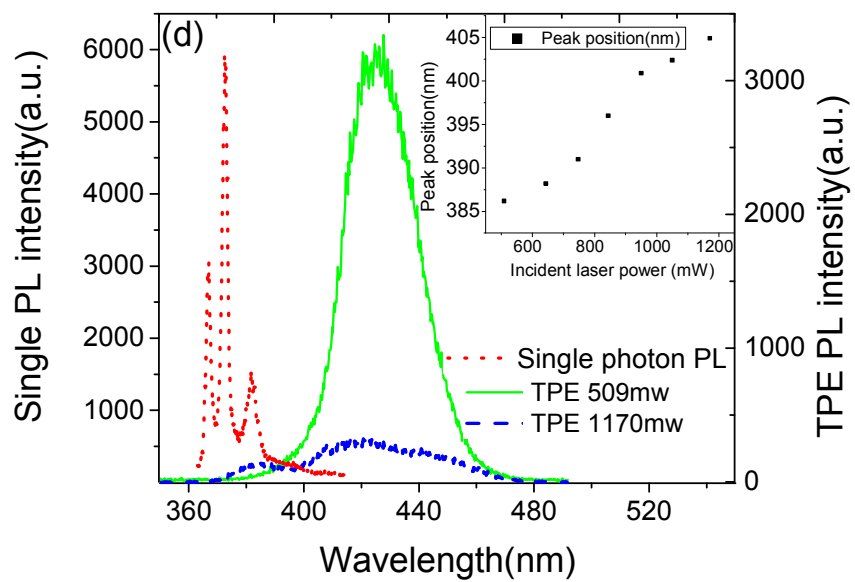


Figure 2: Lin et al.

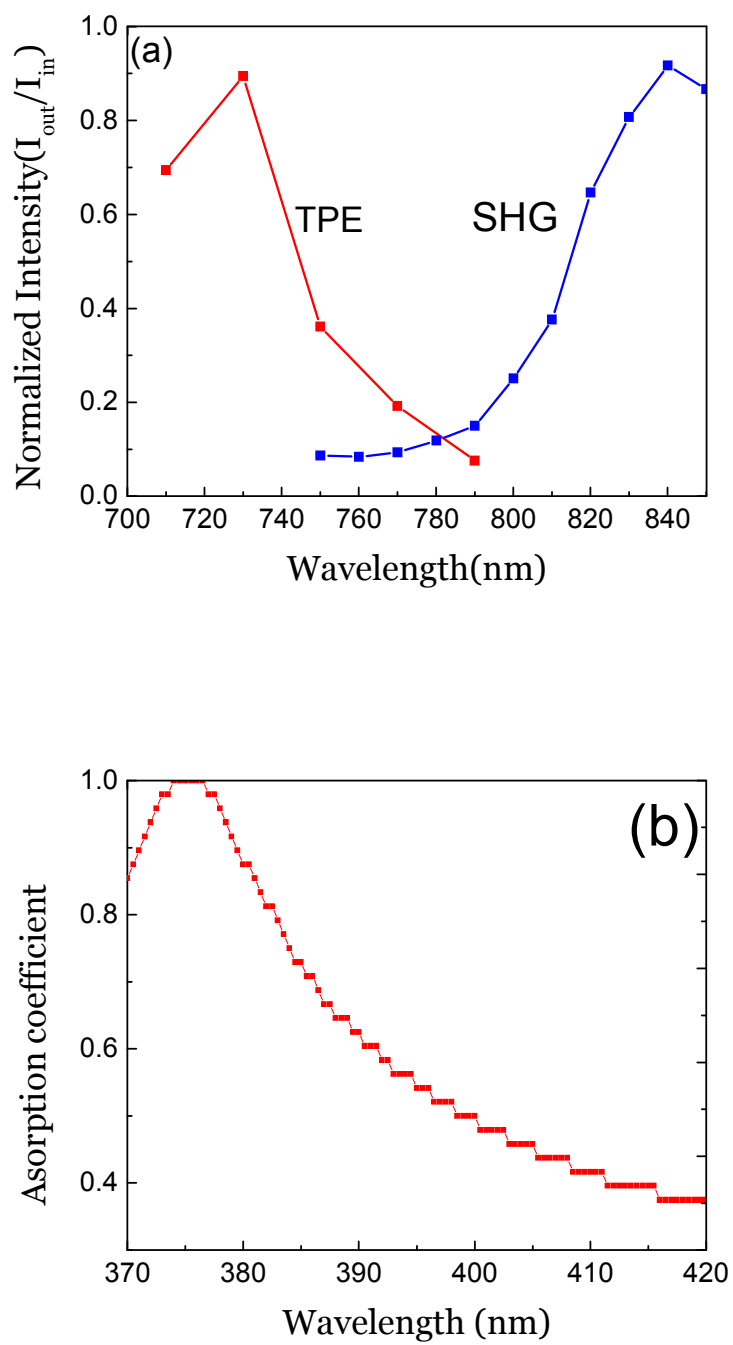


Figure 3: Lin et al.

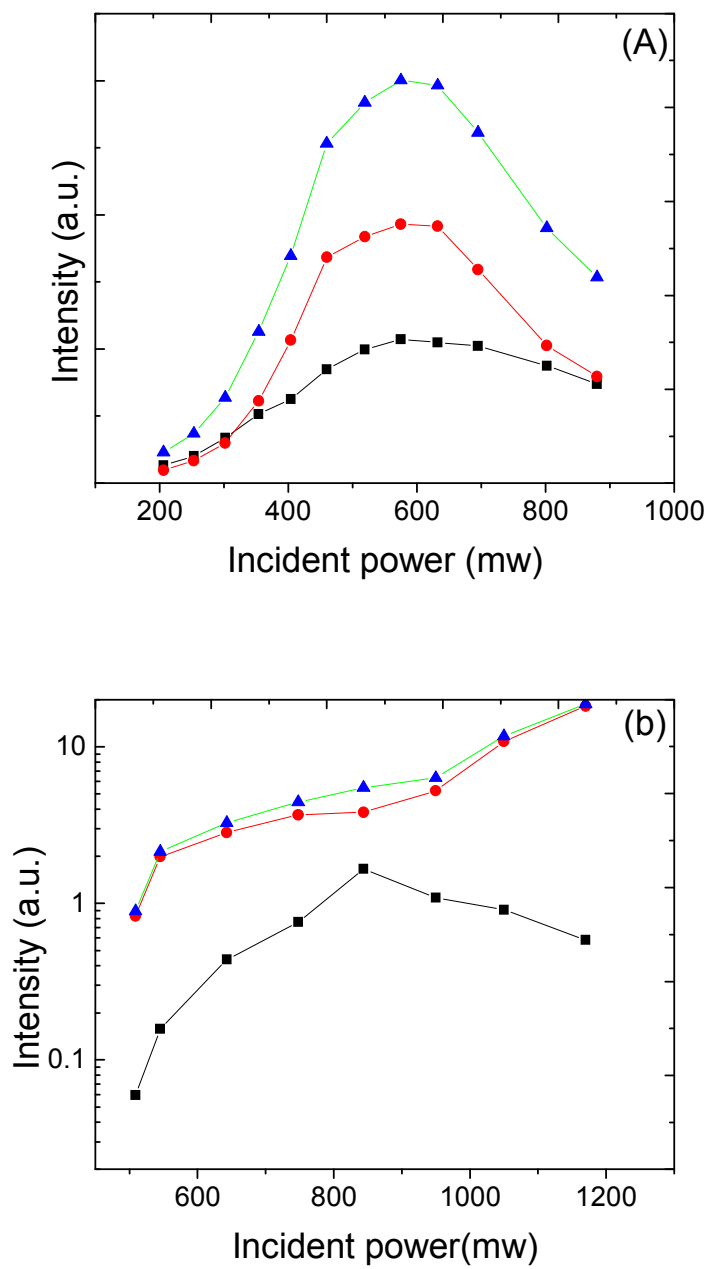


Figure 4: Lin et al.

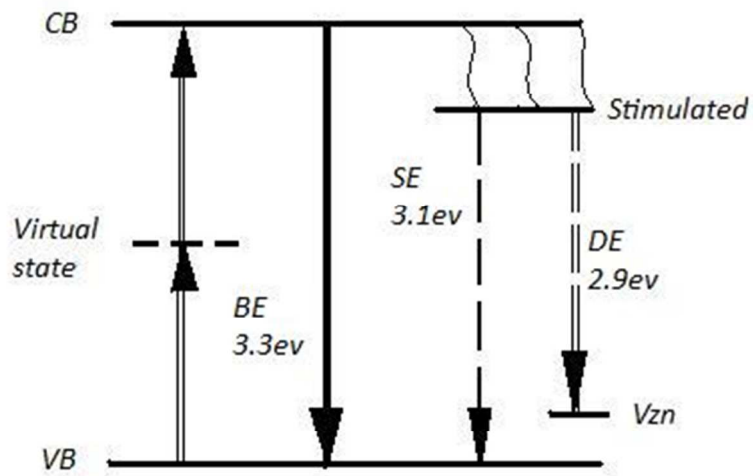


Figure 5: Lin et al.

